FROM FIELD TO GEOPHYSICAL DATA: AN EXAMPLE OF ONGOING FOLD GROWTH FROM THE GREATER CAUCASUS, REPUBLIC OF GEORGIA

F.L. Bonali[1], A. Tibaldi[1], F. Pasquaré Mariotto[3], E. Russo[1], V. Alania[2], A. Chabukiani[2], O. Enukidze[2], N. Tsereteli[2]

[1] Department of Earth and Environmental Sciences, University of Bicocca, Milan, Italy
[2] M. Nodia Institute of Geophysics, M. Javakhishvili State University, Tbilisi, Georgia
[3] Department of Theoretical and Applied Sciences, Insubria University, Varese, Italy

Introduction. Ongoing deformation processes that combine fault propagation and folding are the cause of diffuse seismicity in many areas of the world as well as in the Republic of Georgia (Fig. 1A). In terms of seismic hazard assessment, a deeper understanding of the structural evolution of tectonically active folds and of their evidence at the surface, are of paramount importance. In this study, we present a multidisciplinary analysis of the active Tsaishi anticline fold (TF) (Fig. 1C), resulting in the development of a 3D model that integrates: i) field geomorphological

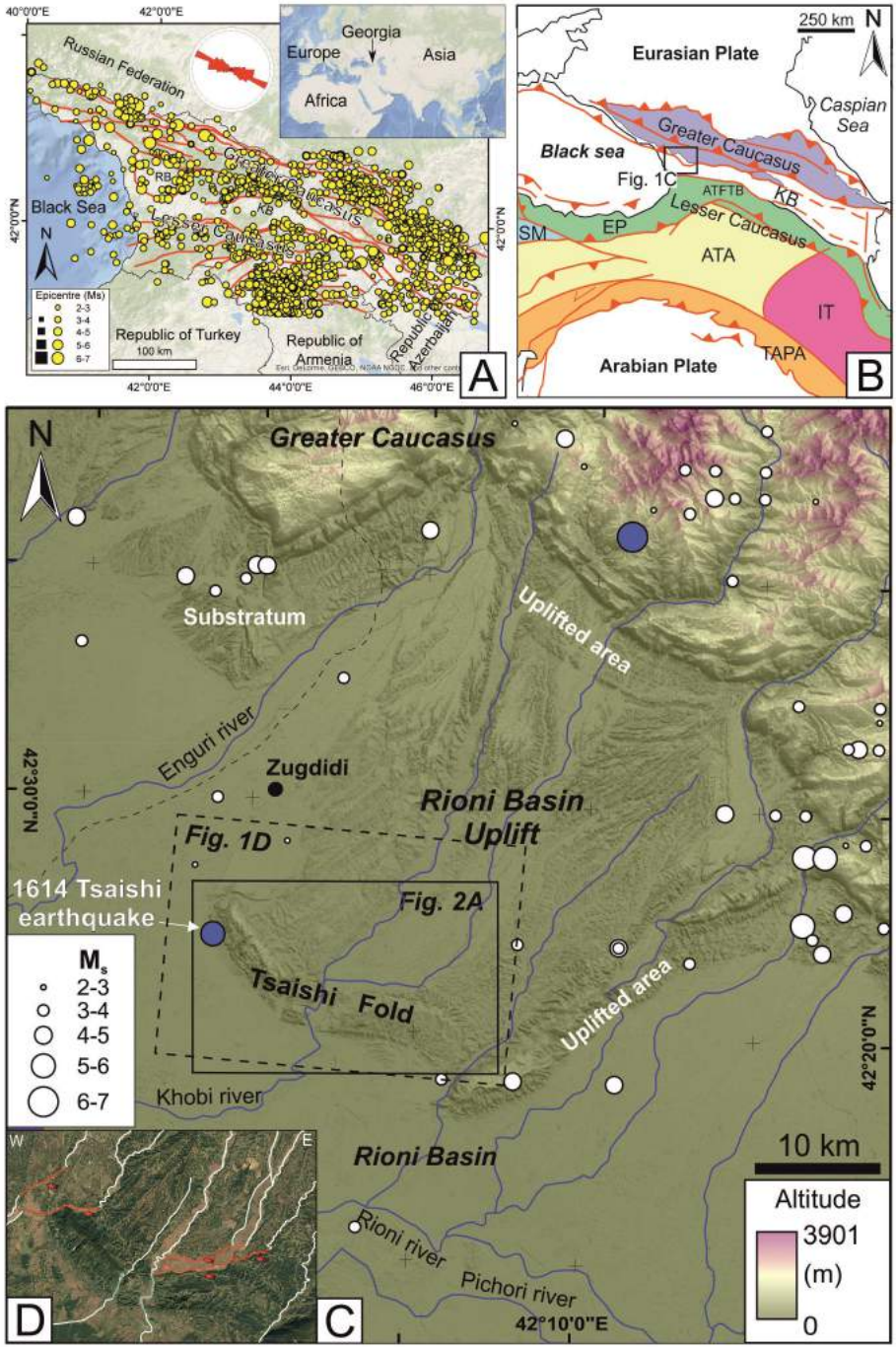

Fig. 1 - A) Active faults and seismicity within the Republic of Georgia (modified after Tsereteli *et al*., 2016). B) Tectonic map of the Arabia-Eurasia collision zone (modified from Sosson *et al*., 2010). Abbreviations: ATFTB-Achara-Trialeti fold and thrust belt; KB-Kura Basin; EP-Eastern Pontides; ATA-Anatolide-Tauride-South Armenian Block; SM-Sakarya massif. C) Rioni Basin uplift area (modified after Tibaldi *et al*., 2017a,b); main rivers and seismicity are reported; white dots represent post-1900 earthquakes (Tsereteli *et al*., 2016) and blue dots are for pre-1900 earthquakes (Varazanashvili *et al*., 2011). D) In figure are shown rivers normally flowing towards the SSW (white lines), which become diverted as they approach the fold (red lines); arrows provide the direction of diversion. The river segments in pale blue indicate the only two cases of rivers crossing the fold.

observations; ii) field geological-structural data; iii) instrumental and historical seismicity; and iv) seismic reflection sections. The studied fold is located in the Western Republic of Georgia, at the south-western tip of the Rioni Basin (RB) uplifted area, at the foothill of Greater Caucasus (Fig 1C). This area is characterized by ongoing mountain building processes, due to collision between the Arabian and Eurasian plates (Fig. 1B) since Tertiary times, as testified by GPS data and by diffuse compressional seismicity, with magnitudes as great as 7 (Tsereteli *et al*., 2016); in particular, the M_S 6.0, 1614 A.D. Tsaishi earthquake occurred just south of the anticline (Fig. 1C, Varazanashvili *et al*., 2011). In accordance with the westward ongoing propagation of the closure of the Transcaucasian depression, the convergence rate between the Greater and the Lesser Caucasus ranges from 4 mm/yr in the RB to the west to 14 mm/yr in the Kura foreland to the east (Reilinger *et al*., 2006). The RB and Kura basins (KB) formed as foreland basins during Oligocene-early Miocene times and were then involved into the orogenic fold and thrust belts (Alania *et al*., 2016 and references therein).

Field and geophysical data. Our field survey has been intended firstly to reconstructing the shallow structure of the TF and to find evidence of recent and still active uplifting, as well as folding and faulting processes. By way of DEM- and field-based geomorphological observations, we observed that the TF crops out for a total length of 29.4 km, taking into account that its NW part seems to be truncated (Fig. 1C and 2A). We also observed that the fold axis trends NW-SE in the western segment, whereas it trends E-W to WNW-ESE in the eastern segment (Fig. 2A).

In the field, we collected a total of 106 measurements of strata attitude along the western segment, and 30 measurements along the eastern segment (Fig. 2A). Regarding the 10-km-long western TF, the northern flank (backlimb) shows dip directions between N00–138° and an average value (Av.) of N45°; dip angles range 5–60° with an Av. of 28°. The southern flank (forelimb) shows dip directions ranging N10–300° with an Av. of N193°; dip angles are between 5° and 89°, the Av. is 46° (Figs. 2). At two sites we observed the presence of overturned strata. This segment can be classified as an asymmetric anticline with a clear vergence to the SW and a NE-dipping axial surface (Schmidt's stereogram in Fig. 2).

In correspondence of the eastern TF, we observed strata attitude changes: dip directions mostly range N2–345° (N70° as Av.) along the northern flank (backlimb), and N119–211° (N179° as Av.) along the southern flank (forelimb) (Fig. 2A). Dip angles are between 5° and 60° (24° as Av.), and 8-60° (22° as Av.) respectively (Fig. 2A). At a general level, the TF can be described as an asymmetric anticline with a clear vergence to the SW and an axial surface dipping to the NE, as shown in the Schmidt's stereogram in Fig. 2A; the field-reconstructed hinge line trends N147° along the NW part, and N125° along the SE part. More to the E, near the Khobi river valley, the hinge line trend changes to about E-W, whereas eastward there is another slight clockwise rotation of strata. In summary, for the eastern part of the TF, from west to east, the hinge line trends N87°, N94° and N110° (Fig. 2A).

Regarding the time evolution of the TF, based on our field observation, the folding process most likely started at the onset of the middle Miocene (e.g. Fig 2B); however, previous authors suggest the possibility of earlier local uplift in the Oligocene. The folding process is presently active, giving rise to a south-vergent anticline, as shown by upwarped late Quaternary river deposits identified in the field. For example, near the NW termination of the TF, there is a series of river terraces of Holocene age, elongated in a NNE-SSW direction (Tibaldi *et al*., 2017a). The surfaces of these terraces show a very shallow dip southward, consistent with the direction of river flow. However, approaching the TF, south of the town of Zugdidi, the dip of the uppermost (i.e. the locally older) terrace surface is northward; some outcrops also show the presence of beds of unconsolidated river conglomerates that dip 7–8° to the north (Fig. 2C), suggesting a very recent uphill tilting of the river deposits. In addition, by observing the plain of the RB near the TF, we noticed that rivers show clear diversions as they approach the TF (red river segments in Fig. 1D), whose growth represented an obstacle to their southward flow.

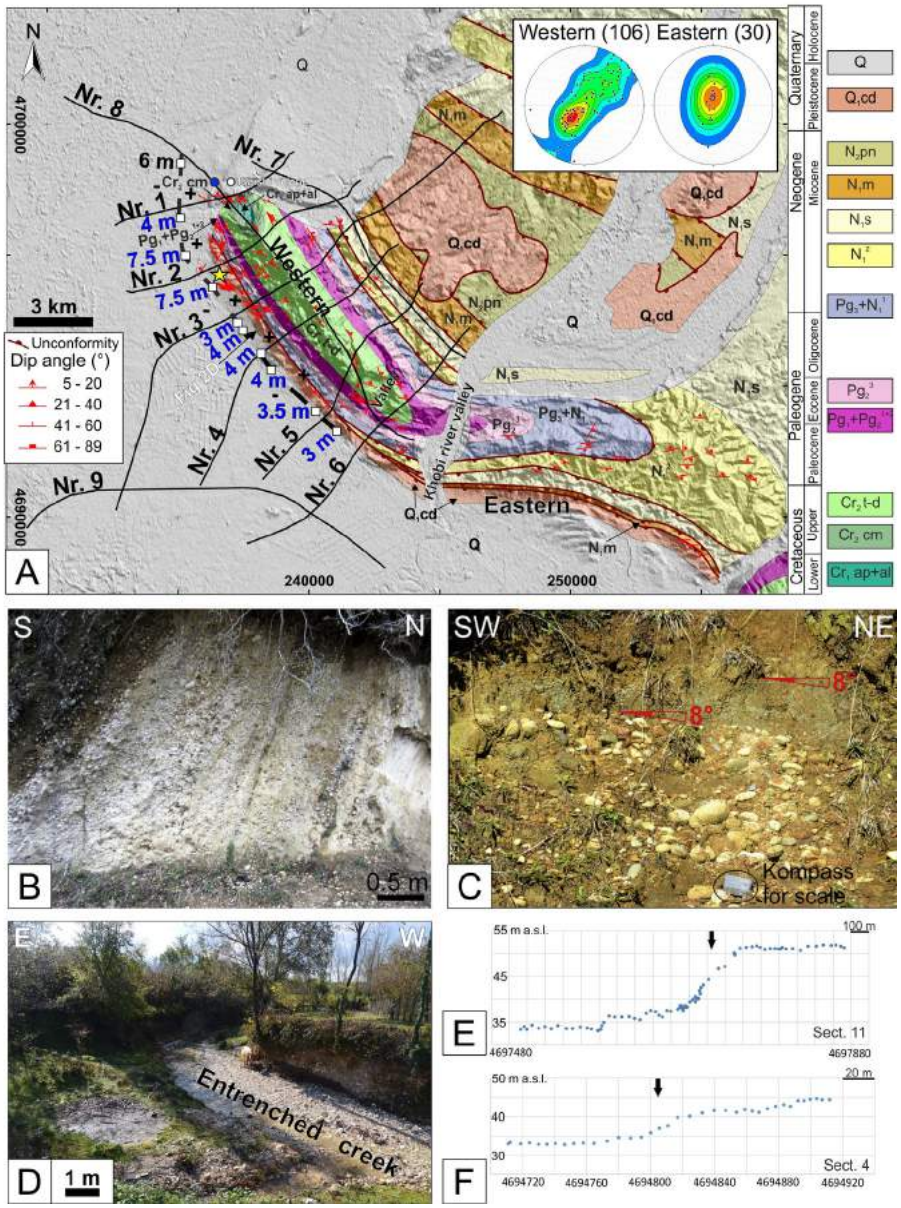

Fig. 2 - Dashed black line: trace of the inferred faults by GPS profiles and field surveys; field and GPS-measured vertical offsets are reported (at white squares); yellow star locates the 1614 A.D. Tsaishi earthquake. (B) Steeply dipping strata, made of conglomerates of Late Miocene age, along the southern flank of the Tsaishi fold (42.395°N, 41.811°E). (C) Photo of river deposits tilted northward; location is provided by the blue dot (D) Example of river stream deeply entrenched immediately north of the fault scarp, i.e. in the hangingwall block. (E-F) Profiles across the fault scarps found at the foothills of the southern flank of the Tsaishi fold (central and SE part). Geological units: Q - Quaternary sediments; Q_1cd -Chaudian (Late Pleistocene) conglomerate and sandstone; N_2pn-Pontian (Upper Miocene) claystone, sandstone and conglomerate; N_1m-Meotian (Upper Miocene) conglomerate, sandstone and claystone; N_1s-Sarmatian (Middle Miocene) claystone, conglomerate and limestone; N_1^2-Middle Miocene claystone, sandstone, marl and limestone; $Pg_3+N_1^1$-Oligocene-beginning of Middle Miocene gypsum bearing claystone, sandstone and marl; Pg_2^3-Upper Eocene marl, basaltic lava, tuff, sandstone, breccias and claystone; $Pg_1+Pg_2^{1+2}$-Paleocene-Lower and Middle Eocene limestone; Cr_2t-d-Turonian-Danian limestone, marl, basaltic lava, tuff, tuff-breccia, sandstone, claystone and limestone; Cr_2cm-Cenomanian sandstone, claystone and limestone; Cr_1ap+al-Aptian-Albian claystone, marl, limestone and sandstone.

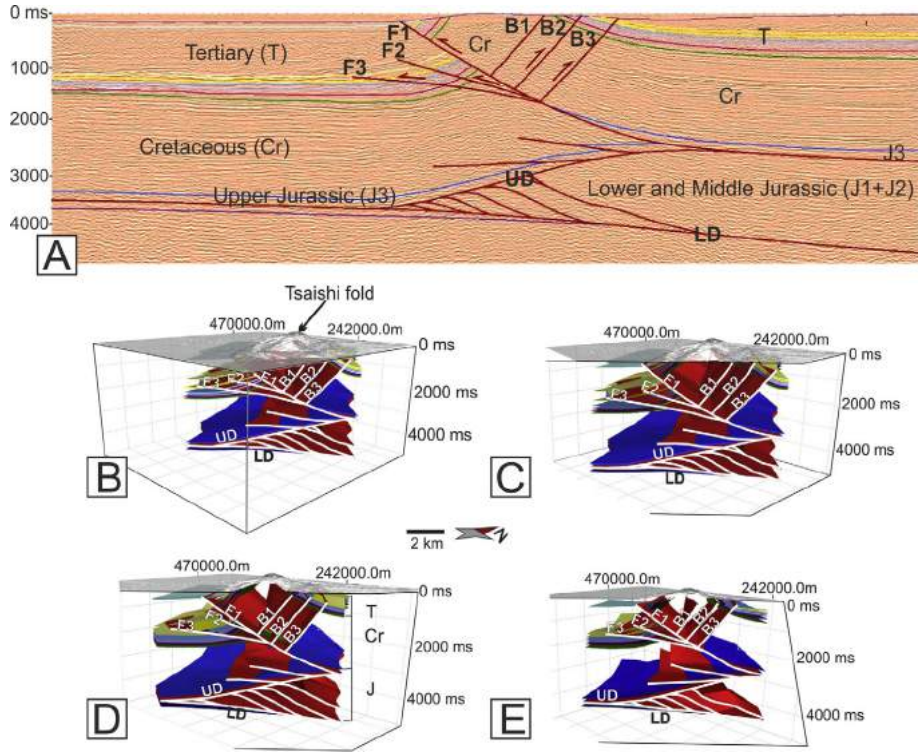

Fig. 3 - A) Interpreted time-migrated seismic reflection sections number 3 (located in Fig. 2A). B-E) 3D reconstruction of the TF, based on seismic reflection sections and field data. Abbreviations: F1, F2 and F3: south-vergent thrust faults; B1, B2 and B3: northvergent backthrusts; UD and LD: upper and lower detachments; T: Tertiary; Cr: Cretaceous; J: Jurassic. Geographic coordinates are shown in UTM WGS84 projection.

Only in two cases the rivers could flow along their original course, in correspondence of the two (already mentioned) NNE-SSW valleys crossing the fold (blue river segments in Figs. 1D and 2A). It is worth noting that these valleys are located exactly in correspondence of the abrupt change in the attitude of the folded strata (e.g. Fig. 2A).

We integrated field observation with the interpretation of seismic reflection sections, with the purpose of reconstructing the general geometry and evolution of the TF. As shown in Fig. 3, the backlimb of the TF is affected by three main backthrusts (faults B1, B2 and B3 in Fig. 3). In regard to the fold's forelimb, at its foot, a main north-dipping thrust has propagated very close to the surface, based on the results of seismic sections (Fig. 3A). Such fault (F1 in Fig. 3) belongs to a fan of reverse low-angle thrusts (comprising F2 and F3 in Fig. 3), as shown in the interpreted seismic section Nr. 3 (see Fig. 2A for location) and in the 3D model (Fig. 3B-E). Lower faults (F2 and F3) cut through a tight syncline and then gradually fade out southward; on the contrary, the shallower fault (F1) seems to crop out at the surface. Through field observation we noticed that, in correspondence of the possible emersion of F1, there is morphological evidence of an almost NW-striking morphological scarp, as high as 7.5 m, measured in the field by tape and GPS profiles (e.g. Fig. 2E-F).

This scarp is 13-km-long (dashed line in Fig. 2A) and may represent the surface fault rupture trace of an active main reverse fault, here named Tsaishi fault, or may represent a fold scarp linked with a very shallow reverse fault. Furthermore, the area immediately north of the inferred scarp is affected by a number of small water streams characterized by entrenching due to intense erosion (e.g. Fig. 2D); the gully in Fig. 2D is 2 meters lower than the surrounding topography. Once the creeks have flowed through the scarp, they suddenly changed their morphology to a

meandering pattern without any erosive processes. The described features are consistent with recent uplift of the area north of the scarp. Finally, the location of the scarp and the related fault geometry are compatible with the historic M_S 6.0 1614 A.D. Tsaishi earthquake, which attests to the seismic hazard of the area. Based on field and geophysical data, we classified the TF as an active fault-propagation fold and we also recognized very recent growing activity associated with a major, underlying active fault. As a result, our work also represents an important contribution to the seismic hazard assessment of the RB, densely-populated area.

Acknowledgements This study has been carried out in the framework of the NATO project SfP G4934 "Georgia Hydropower Security", of the International Lithosphere Program - Task Force II, and of the European Space Agency project n. 32309 "Active tectonics and seismic hazard of southwest Caucasus by remotely-sensed and seismological data". Seismic sections were kindly made available by the State Agency for Regulation of Oil and Gas Resources of Georgia (SAROGR).

References

Alania, V., Chabukiani, A., Chagelishvili, R., Enukidze, O., Gogrichiani, K., Razmadze, A., Tsereteli, N., 2016. Growth structures, piggyback basins and growth strata of Georgian part of Kura foreland fold and thrust belt: implication for Late Alpine kinematic evolution. In: Sosson, M., Stephenson, R., Adamia, Sh. (Eds.), Tectonic Evolution of the Eastern Black Sea and Caucasus. Geological Society of London, Special Publications No. 428: p. 810 http://dx.doi.org/10.1144/SP428.5 (first published on October 27, 2015).

Reilinger, R.E.,McClusky, S.C., Vernant, P., Lawrence, S., Ergintav, S., Cakmak, R., Ozener, H., Kadirov, F., Guliev, I., Stepanian, R., Nadariya, M., Hahubia, G., Mahmoud, S., Sakr, K., Arrajehi, A., Paradissis, D., Al-Aydrus, A., Prilepin, M., Guseva, T., Evren, E., Dmirotsa, A., Filikov, S.V., Gomez, F., Al-Ghazzi, R., Karam, G., 2006. GPS constraints on continental deformation in the Africa-Arabia-Eurasia continental collision zone and implications for the dynamics of plate interactions.

Sosson, M., Rolland, Y., Danelian, T., Muller, C., Melkonyan, R., Adamia, S., Kangarli, T., Avagyan, A., Galoyan, G., 2010. Subductions, obduction and collision in the Lesser Caucasus (Armenia Azerbaijan, Georgia), new insights. In: Sosson, M., Kaymakci, N., Stephanson, R., Bergarat, F., Storatchenoko, V. (Eds.), Sedimentary Basin TectonicsFrom the Black Sea and Caucasus to the Arabian Platform. Geological Society of London Special Publication 340, pp. 329–352.

Tibaldi, A., Alania, V., Bonali, F.L., Enukidze, O., Tsereteli, N., Kvavadze, N., Varazanashvili, O., 2017a. Active inversion tectonics, simple shear folding and back-thrusting at Rioni Basin, Georgia. J. Struct. Geol. 96, 35–53.

Tibaldi, A., Russo, E., Bonali, F. L., Alania, V., Chabukiani, A., Enukidze, O., & Tsereteli, N., 2017b. 3-D anatomy of an active fault-propagation fold: A multidisciplinary case study from Tsaishi, western Caucasus (Georgia). Tectonophysics.

Tsereteli, N., Tibaldi, A., Alania, V., Gventsadse, A., Enukidze, O., Varazanashvili, O., Müller, B.I.R., 2016. Active tectonics of central-western Caucasus, Georgia. Tectonophysics

Varazanashvili, O., Tsereteli, N., Tsereteli, E., 2011. Historical Earthquakes in Georgia (up to 1900): Source Analysis and Catalogue Compilation. Monograph. M. Javakhishvili Tbilisi State University, Georgia.